

## High Field Phase Diagram of Cuprates Derived from the Nernst Effect

Yayu Wang,<sup>1</sup> N.P. Ong,<sup>1</sup> Z. A. Xu,<sup>1,\*</sup> T. Kakeshita,<sup>2</sup> S. Uchida,<sup>2</sup> D. A. Bonn,<sup>3</sup> R. Liang,<sup>3</sup> and W. N. Hardy<sup>3</sup>

<sup>1</sup>*Department of Physics, Princeton University, Princeton, New Jersey 08544*

<sup>2</sup>*School of Frontier Sciences, University of Tokyo, Bunkyo-ku, Tokyo 113-8656, Japan*

<sup>3</sup>*Department of Physics and Astronomy, University of British Columbia, Vancouver, British Columbia, Canada V6T 1Z1*

(Received 30 January 2002; published 7 June 2002)

Measurements of the Nernst signal in the vortex-liquid state of the cuprates to high fields (33 T) reveal that vorticity extends to very high fields even close to the zero-field critical temperature  $T_{c0}$ . In overdoped  $\text{La}_{2-x}\text{Sr}_x\text{CuO}_4$ , we show that the upper critical field  $H_{c2}(T)$  curve does not end at  $T_{c0}$ , but at a much higher temperature. These results imply that  $T_{c0}$  corresponds to a loss in phase rigidity rather than a vanishing of the pairing amplitude. An intermediate field  $H^*(T) \ll H_{c2}(T)$  is shown to be the field scale for the flux-flow resistivity.

DOI: 10.1103/PhysRevLett.88.257003

PACS numbers: 74.40.+k, 72.15.Jf, 74.25.Fy, 74.72.-h

In the cuprate superconductors, strong fluctuations of the order parameter [1,2] and the extreme field scales make the task of constructing the experimental phase diagram a formidable challenge. While the important vortex-solid melting line  $H_m(T)$  is now well known [3–5], there is great uncertainty in the region above  $H_m$ . A key difficulty is the *loss of long-range phase rigidity* in the transition to the vortex-liquid state. In the vortex-liquid state, the flux-flow resistivity  $\rho$  rises very rapidly to the (extrapolated) normal-state value [6] even though substantial condensate strength and pairing amplitude remain. This makes  $\rho$  an unreliable “diagnostic” of the field suppression of the pairing amplitude. By contrast, the Nernst and Ettinghausen effects can probe the existence of vorticity in the superfluid with undiminished sensitivity even in intense fields. From Nernst measurements in  $\text{La}_{2-x}\text{Sr}_x\text{CuO}_4$  (LSCO) and  $\text{YBa}_2\text{Cu}_3\text{O}_y$  (YBCO) in fields up to 33 T, we have uncovered an anomalous property of  $H_{c2}(T)$  near their zero-field critical temperature  $T_{c0}$ . This anomaly is related to the existence of vortexlike excitations high above  $T_{c0}$  [7,8], and is central to the key question of whether the Meissner transition in zero field is caused by the collapse of long-range phase coherence or the vanishing of the pairing amplitude (see also Corson *et al.* [9]). In YBCO, previous Ettinghausen [10] and Nernst [11,12] measurements were performed in lower fields. Measurements on LSCO have been extended recently to high fields [13].

In the Nernst experiment, vortices moving with velocity  $\mathbf{v}$  down a thermal gradient  $-\nabla T \parallel \hat{\mathbf{x}}$  generate a Josephson voltage which is observed as a transverse  $E$ -field  $E_y = Bv_x$ , with  $\mathbf{B}$  the mean flux density. The vortex-Nernst effect is well explored in low- $T_c$  superconductors. Figure 1b shows the Ettinghausen-Nernst effect in  $\text{PbIn}$  [14]. The depinning of the vortex lattice by a supercurrent ( $\mathbf{J} \parallel \hat{\mathbf{x}}$ ) leads to a large transverse heat current  $J_y^h \parallel \hat{\mathbf{y}}$  that rises to a maximum and then decreases to zero at  $H_{c2}$  (the weak fluctuation tail above  $H_{c2}$  is not relevant here). By Onsager reciprocity, the Nernst signal  $e_y \equiv E_y/|\nabla T|$  shares the same profile as  $J_y^h$  in Fig. 1b [15]. To compare with theory,  $e_y$  is divided by  $\rho(H)$  to obtain the “transport

line-entropy”  $s_\phi = \phi_0 e_y / \rho$  ( $Ts_\phi$  is the heat energy carried by a unit-length vortex line). In  $\text{PbIn}$ , the linear decrease in  $s_\phi$  near  $H_{c2}$  matches that of the magnetization  $M(T, H) = -[H_{c2}(T) - H]/1.16[2\kappa^2 - 1]$  ( $\kappa$  is the Ginzburg-Landau parameter), as given by the Caroli-Maki expression [14,16],

$$s_\phi(T, H) = \frac{\phi_0}{T} |M(T, H)| L_D(T) \quad (1)$$

[here  $L_D(T)$  decreases gradually with  $T$  from 1 at  $T_{c0}$ ].

We start with the overdoped regime, where the field profiles of  $e_y$  most resemble those in  $\text{PbIn}$ . In Fig. 1a, we display curves of  $e_y$  vs field  $H$  in sample 1 ( $\text{La}_{2-x}\text{Sr}_x\text{CuO}_4$  with  $x = 0.20$  and  $T_{c0} = 28$  K) (for experimental details, see Ref. [8]). At each temperature  $T$ , the signal rises steeply above  $H_m$ , attaining a prominent maximum before decreasing. The total data set defines experimentally the region in  $H$  and  $T$  where vorticity is strongly present. As in  $\text{PbIn}$ , the monotonic decrease at high fields reflects the field suppression of the condensate strength. At high fields, all the curves below 14 K are observed to follow a common curve towards zero (dashed line). The trend implies that the low- $T$  traces are all wedged between the field axis and the broken line. Hence all the low- $T$  curves vanish at the intercept of the common curve with the field axis (45–50 T), which corresponds to  $H_{c2}(0)$ .

Going to higher  $T$ , we immediately encounter an anomaly. Conventionally, the  $H_{c2}$  line goes linearly to zero at  $T_{c0}$ . Hence,  $e_y$  ought to be finite in a field interval that  $\rightarrow 0$  as  $T \rightarrow T_{c0}^-$ . In sharp contrast, we find that, close to  $T_{c0}$ , the magnitude of  $e_y$  remains large and nearly unchanged up to intense fields. There is no evidence for a field scale (flagged by  $e_y \rightarrow 0$ ) that decreases to zero regardless of how close we are to  $T_{c0}$ . To make this point quantitative, we convert  $e_y$  to  $s_\phi$  using  $\rho(T, H)$  measured in the same sample. The line entropy rises steeply to a sharp maximum before decreasing monotonically (Fig. 1c). The linear decrease at high fields, strikingly similar to that in  $\text{PbIn}$ , allows  $H_{c2}(T)$  to be determined [17]. These results

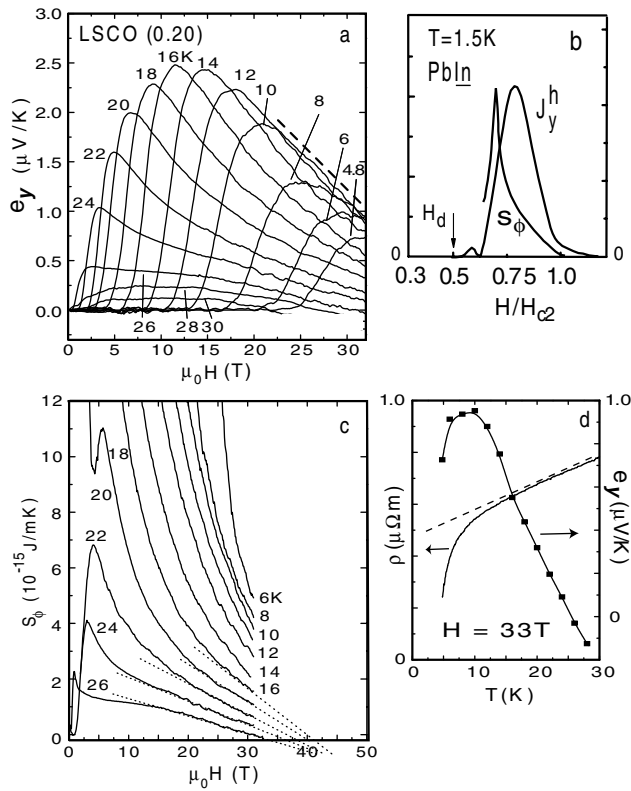


FIG. 1. (a) The field dependence of  $e_y \equiv E_y/|\nabla T|$  at indicated  $T$  in sample 1 (LSCO with  $x = 0.20$ ,  $T_{c0} = 28$  K). Below 25 K,  $e_y$  rises to a sharp peak before decreasing monotonically. The dashed line indicates asymptotic behavior at large- $H$  and low- $T$ . (b) Plots of the transverse heat flux  $J_y^h$  and  $s_\phi$  vs  $H$  in an Ettinghausen experiment in PbIn at 1.5 K (by reciprocity,  $J_y^h = e_y/JT$ , with  $J$  the applied supercurrent).  $H_d$  is the depinning field (modified from Vidal [14(a)]). (c) The field dependence of the transport line entropy  $s_\phi$  obtained from  $e_y$  and  $\rho$  in sample 1 (LSCO,  $x = 0.20$ ). The high-field linear extrapolations (dotted lines) provide estimates of  $H_{c2}(T)$ . Fits to Eq. (1) give  $\kappa = 670$  and 500 at 26 and 18 K, respectively. (d) The temperature dependence of  $\rho$  and  $e_y$  in sample 1 in a fixed field (33 T). The dashed line is the extrapolation of  $\rho_N$ . Note that  $e_y$  (measured at 33 T) goes to zero at  $\sim 26$  K instead of  $\sim 9$  K (the “knee” in  $\rho$ ).

show that  $H_{c2}(T)$  decreases with rising  $T$ , but remains at extraordinarily high values as  $T \rightarrow T_{c0}$  (see Fig. 2). [We neglect a small correction from the negative Nernst coefficient  $v_N \approx -40$  nV/KT of the holes in overdoped LSCO (Fig. 3 of Ref. [7]). Accounting for the background increases  $s_\phi$  and  $H_{c2}(T)$  by  $\sim 10\%$ .]

A powerful way to summarize the anomalous trends described is to represent  $e_y(T, H)$  as a contour plot in the  $T$ - $H$  plane (Fig. 2). In the vortex-solid phase below the melting line  $H_m$  (lower white curve),  $e_y = 0$  because the vortices are pinned. As the vortex solid melts across  $H_m$ ,  $e_y$  increases steeply up to the “ridge” which represents a field scale that we call  $H^*(T)$  (upper white curve). To the right of the ridge,  $e_y$  falls monotonically. We focus on the two interesting regimes: the low- $T$  limit and the region near  $T_{c0}$ .

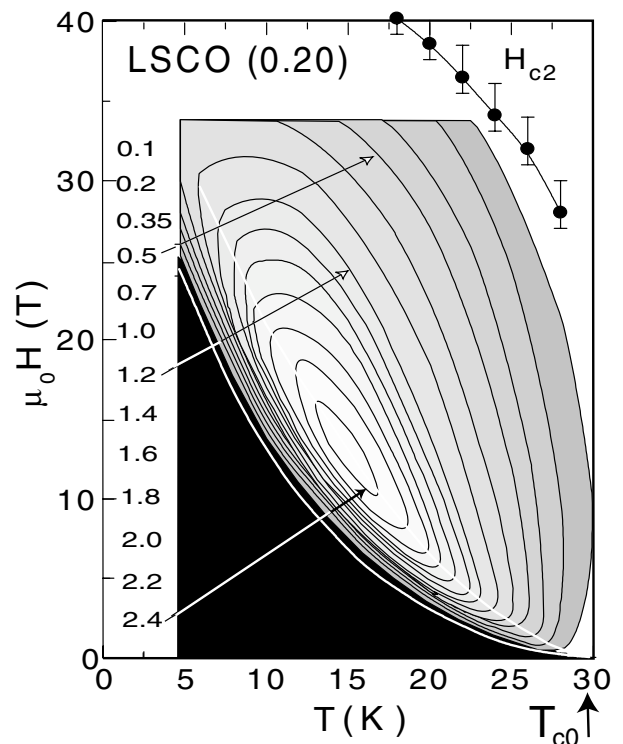


FIG. 2. The measured values of  $e_y(T, H)$  in sample 1 (LSCO,  $x = 0.20$ ) represented as a contour plot in the  $T$ - $H$  plane. Values of  $e_y$  (in  $\mu\text{V}/\text{K}$ ) at successive contour lines are shown on the left column (white arrows). The lower and upper white lines are the melting field  $H_m$  and “ridge” field  $H^*$ , respectively.  $H_{c2}(T)$  values estimated from Fig. 1c are shown as solid circles.  $T_{c0}$  is indicated in the lower-right corner.

As  $T \rightarrow 0$ , the two fields  $H_m(T)$  and  $H^*(T)$  increase rapidly towards values approaching  $H_{c2}(0)$  [18]. In this large- $H$ , low- $T$  region, the contours are nearly horizontal, as required by the asymptotic high-field behavior (broken curve in Fig. 1a). This implies that the  $H_{c2}$  line is nearly horizontal below  $\sim 12$  K, as anticipated above. At temperatures  $T \leq T_{c0}$ , the weak attenuation of  $e_y$  to high fields corresponds to the nearly vertical orientation of the contours. Clearly, there is no evidence for a putative  $H_{c2}$  line that terminates at  $T_{c0}$ . The values of  $H_{c2}(T)$  derived from  $s_\phi$  are plotted in Fig. 2 as solid circles.

The anomalous features of the Nernst signal become more pronounced when we go to the underdoped regime. A major change from the overdoped case is apparent in the field profiles of  $e_y$ . We show in Fig. 3 results in underdoped YBCO (sample 2, with  $y = 6.50$  and  $T_{c0} = 50$  K). As  $H$  increases above  $H_m$ ,  $e_y$  rises rapidly, but attains a very broad maximum that extends undiminished to 30 T. In comparison with the curves in Fig. 1a, we see that  $e_y$  in sample 2 approaches zero only at fields considerably higher than 30 T. If we now convert  $e_y$  to  $s_\phi$  using the measured  $\rho$ , the broad profile translates to a line entropy that extrapolates to zero at fields much higher than our maximum field. At 40 K, we may estimate the lower

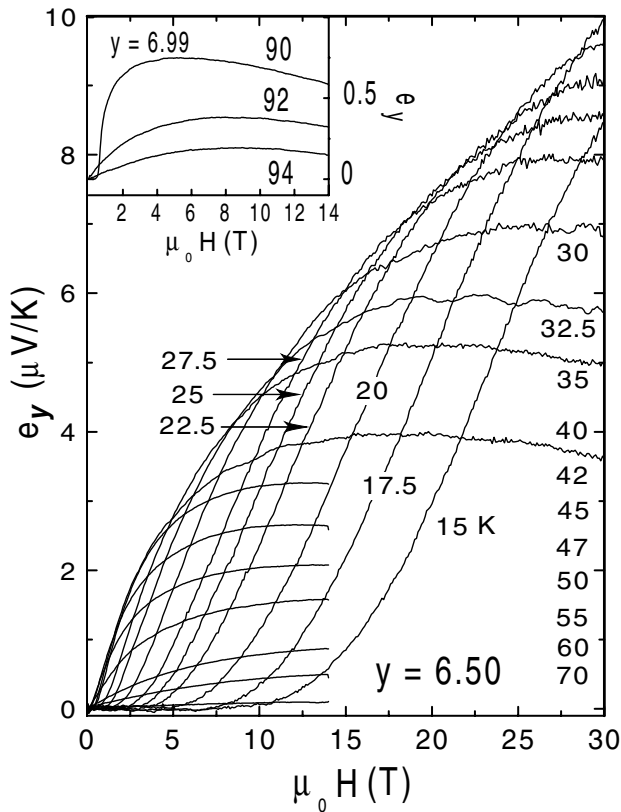


FIG. 3. Variation of the Nernst signal  $e_y \equiv E_y/|\nabla T|$  with field  $H$  at fixed  $T$  in sample 2 (YBCO with  $y = 6.50$ ,  $T_{c0} = 50$  K). Above 40 K, the measurements were performed up to 14 T only. The inset shows  $e_y$  vs  $H$  in sample 3 (YBCO,  $y = 6.99$ ) close to its  $T_{c0} = 93$  K. Both are detwinned crystals grown in barium zirconate crucibles.

bound  $H_{c2}(T) \geq 60$  T, which is very high for a temperature so close to  $T_{c0} = 50$  K. These features are common to all the underdoped cuprates we have investigated until now (for results in LSCO and Bi 2201, see Ref. [8]).

The contour plot of  $e_y$  for sample 2 is displayed in the main panel of Fig. 4. In comparison with Fig. 2, the melting line is now considerably lower relative to  $H^*$ . Further, the contour lines in the region around  $T_{c0}$  are more spread out. The Nernst signal retains considerable strength at 70 K, indicating that vorticity strongly persists up to 20 K above  $T_{c0}$ . The contour plots show rather clearly the continuity between the high-temperature fluctuation phase observed by Xu *et al.* [7,8] and the vortex-liquid state below  $T_{c0}$ . The two regimes smoothly merge together, and no phase boundary or “crossover” line separating them is apparent in the  $T$ - $H$  plane. As mentioned above, the upper critical field is estimated to be above 60 T even at 40 K. The much higher field scale in underdoped YBCO is also apparent if we compare the contour plots in Figs. 2 and 4. In overdoped LSCO, the contours close at fields above 13 T (the field scale of the “island”), whereas, in underdoped YBCO, they do not close until  $H$  exceeds 30 T. For comparison, we also display the contours in near-

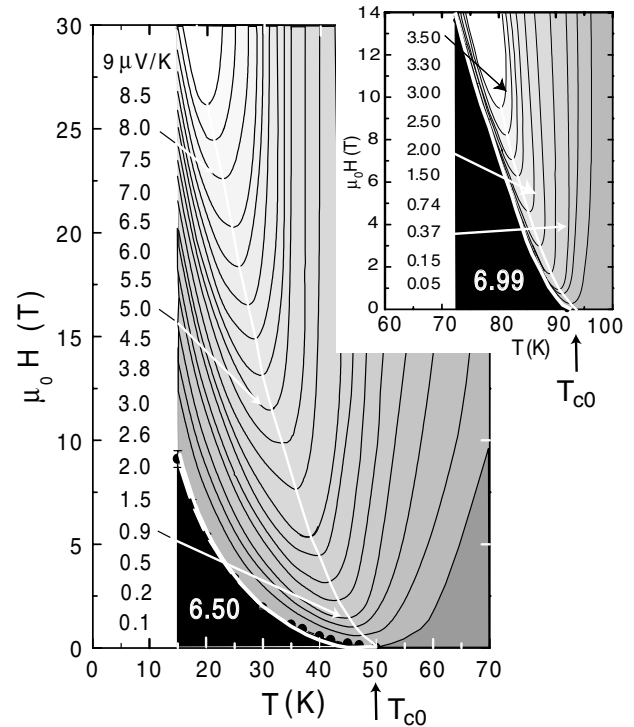


FIG. 4. (Main panel) Contour plot of  $e_y$  in the  $T$ - $H$  plane in sample 2 (YBCO,  $y = 6.50$ ). The upper (lower) white curve represents the “ridge” field  $H^*$  (melting field  $H_m$ ). Inset shows the corresponding contour plot in sample 3 ( $y = 6.99$ ). Note that the region between  $H_m$  and  $H^*$  is compressed to a thin sliver.

optimal YBCO (sample 3 with  $y = 6.99$  and  $T_{c0} = 93$  K). As shown by the vertical orientation of the contour lines from 85 to 95 K, as well as the field profiles in the inset in Fig. 3,  $e_y$  is virtually field independent up to 14 T. Even for near-optimal YBCO, there is no evidence for an  $H_{c2}$  line that decreases to zero at  $T_{c0}$  (this calls into question the interpretation of “ $H_{c2}$ ” values inferred from bulk magnetization results [19]).

The observation of vortexlike excitations high above  $T_{c0}$  by Xu *et al.* [7,8] raised the question of whether the cuprate superconducting transition at  $T_{c0}$  actually corresponds to the loss of long-range phase rigidity, as opposed to the vanishing of the Gorkov pairing amplitude  $\mathcal{F}(\mathbf{x}, \mathbf{x}')$  [20]. The present results provide strong support for the former. A prominent anomaly at temperatures near  $T_{c0}$  is the remarkably weak field dependence of  $e_y$  above the field scale  $H^*(T)$ , which implies that the condensate strength extends undiminished to very high fields. In underdoped cuprates, this anomalous behavior persists to our lowest temperatures (Fig. 3). However, in overdoped samples, the profiles sharpen up below 25 K to reveal pronounced field suppression at high fields (Fig. 1a). Values of  $H_{c2}(T)$  inferred from the line-entropy profiles show that the reason for the anomaly is that the  $H_{c2}$  vs  $T$  line does not terminate at  $T_{c0}$ , but at a much higher temperature.

This seems to us to be compelling evidence that, at  $T_{c0}$ , the steep increase of  $\rho$  and the collapse of the Meissner effect correspond to a preemptive loss of phase rigidity (as has been advocated by Emery and Kivelson, and the early resonating valence bond theory [20]) rather than the vanishing of  $\mathcal{F}(\mathbf{x}, x')$ . This scenario is qualitatively distinct from that in bulk low- $T_c$  superconductors. Although  $\rho$  saturates rapidly to  $\rho_N$  above  $T_{c0}$  (in zero field), there remains sufficient condensate density to support vorticity. In sample 1, the measured  $H_{c2}$  curve implies that we need to apply fields above 30 T to suppress all vorticity near  $T_{c0}$ . The field scale is even higher in underdoped YBCO.

A hallmark of the vortex-liquid state in cuprates is that  $\rho$  rapidly increases and “saturates” to the extrapolated normal-state value ( $\rho_N$ ) even when  $H \ll H_{c2}(T)$ . To illustrate this, we plot the  $T$  dependence of  $\rho$  and  $e_y$  in sample 1 with  $H$  fixed at 33 T in Fig. 1d (inset). Clearly, the large Nernst signal indicates that the region from 5 to 25 K is in the vortex-liquid state (see Fig. 2). However, between 15 and 30 K,  $\rho$  virtually lies on the extrapolated  $\rho_N$  curve. Hence, reliance on  $\rho$  alone would lead to a serious underestimate of  $H_{c2}$ .

In all cuprates studied, the ridge field  $H^*(T)$  line is ubiquitous. Over a broad range of  $T$ , the ratio  $\rho/\rho_N$  has the value 0.3–0.4 on the curve  $H^*$  vs  $T$ .  $H^*(T)$  serves as the boundary separating the low-field regime in which  $\rho$  rapidly increases with  $H$ , from the high-field regime in which  $\rho$  slowly asymptotes to the extrapolated  $\rho_N$ . Hence,  $H^*$  represents an intrinsic field scale that controls dissipation in the vortex liquid state (attempts to find  $H_{c2}$  using  $\rho$  alone invariably turn up a curve akin to  $H^*$  rather than the higher  $H_{c2}$ ). If we identify a length scale  $\xi^*(T)$  by the ratio  $\xi^*(T)/\xi_0(T) \sim \sqrt{H_{c2}(T)/H^*(T)}$ , we find that, at low  $T$ ,  $\xi^*/\xi_0 \approx 1$ . As  $T$  increases, however, the ratio rapidly increases (to 1.8 and 3.7 at 15 and 25 K, respectively). Since  $H^*$  determines the onset of strong flux-flow dissipation,  $\xi^*$  represents a radius larger than the vortex core radius  $\xi_0$  ( $\approx 2.6$  nm). Packing vortices closer than the outer radius  $\xi^*$  leads to a crossover to the high-dissipation state in which  $\rho$  asymptotes to  $\rho_N$ . However, as superfluidity and its associated  $2\pi$  phase winding survive right up to the inner radius  $\xi_0$  [21], the Nernst signal is observable to the higher field scale  $H_{c2}$  ( $s_\phi$  is strongly attenuated in magnitude because of the reduced supercurrent for  $\xi^* < r < \xi_0$ ) [17]. A length scale extending outside the vortex core has been observed in tunneling experiments [22].

We thank S. Hannahs for valuable assistance at the National High Magnetic Field Laboratory (a facility supported by NSF and the state of Florida). We acknowledge useful discussions with P.W. Anderson, A.J. Millis, and Z.Y. Weng. This research is supported by a NSF grant (NSF-DMR 98-09483), the Office of Naval Research (N00014-01-0281), the New Energy and Industrial Technology Development Organization (NEDO), Japan, the

Natural Sciences and Engineering Research Council, and the Canadian Institute for Advanced Research.

\*Present address: Department of Physics, Zhejiang University, Hangzhou, China.

- [1] D. S. Fisher, M. P. A. Fisher, and D. A. Huse, *Phys. Rev. B* **43**, 130 (1991).
- [2] G. Blatter, M. V. Feigel'man, V. B. Geshkenbein, A. I. Larkin, and V. M. Vinokur, *Rev. Mod. Phys.* **66**, 1125 (1994).
- [3] E. Zeldov, D. Majer, M. Konczykowski, V. B. Geshkenbein, V. M. Vinokur, and H. Shtrikman, *Nature (London)* **375**, 373 (1995).
- [4] A. Schilling, R. A. Fisher, N. E. Phillips, U. Welp, D. Dasgupta, W. K. Kwok, and G. W. Crabtree, *Nature (London)* **382**, 791 (1996).
- [5] R. Liang, D. A. Bonn, and W. N. Hardy, *Phys. Rev. Lett.* **76**, 835 (1996).
- [6] See, e.g., T. R. Chien, T. W. Jing, N. P. Ong, and Z. Z. Wang, *Phys. Rev. Lett.* **66**, 3075 (1991).
- [7] Z. A. Xu, N. P. Ong, Y. Wang, T. Kakeshita, and S. Uchida, *Nature (London)* **406**, 486 (2000).
- [8] Yayu Wang, Z. A. Xu, T. Kakeshita, S. Uchida, S. Ono, Yoichi Ando, and N. P. Ong, *Phys. Rev. B* **64**, 224519 (2001).
- [9] J. Corson, R. Mallozzi, J. Orenstein, J. N. Eckstein, and I. Bozovic, *Nature (London)* **398**, 221 (1999).
- [10] T. T. M. Palstra, B. Batlogg, L. F. Schneemeyer, and J. V. Waszczak, *Phys. Rev. Lett.* **64**, 3090 (1990).
- [11] H. C. Ri, R. Gross, F. Gollnik, A. Beck, R. P. Huebener, P. Wagner, and H. Adrian, *Phys. Rev. B* **50**, 3312 (1994).
- [12] J. A. Clayhold, A. Linnen, F. Chen, and C. W. Chu, *Phys. Rev. B* **50**, 4252 (1994).
- [13] C. Capan *et al.*, *Phys. Rev. Lett.* **88**, 056601 (2002).
- [14] Felix Vidal, *Phys. Rev. B* **8**, 1982 (1973); O. L. de Lange and F. A. Otter, Jr., *J. Low Temp. Phys.* **18**, 31 (1975); R. P. Huebener and A. Seher, *Phys. Rev.* **181**, 701 (1969).
- [15] The constitutive equations and Onsager reciprocity are discussed in Refs. [16].
- [16] C. Caroli and K. Maki, *Phys. Rev.* **164**, 591 (1967); A. Houghton and K. Maki, *Phys. Rev. B* **3**, 1625 (1971); Chia-Ren Hu, *Phys. Rev. B* **13**, 4780 (1976).
- [17] Figure 1c shows why previous attempts to fit Eq. (1) to curves of  $Ts_\phi$  vs  $T$  (taken at fixed  $H < 15$  T) were problematical. The data lie outside the regime of the perturbation calculation.
- [18] Below 16 K in LSCO,  $H_m(T) \sim e^{-T/T_0}$  with  $T_0 \approx 6$  K. Similar behavior of  $H_m$  is seen in underdoped YBCO.
- [19] U. Welp *et al.*, *Phys. Rev. Lett.* **62**, 1908 (1989).
- [20] V. J. Emery and S. A. Kivelson, *Nature (London)* **374**, 434 (1995); G. Baskaran, Z. Zou, and P. W. Anderson, *Solid State Commun.* **63**, 973 (1987).
- [21] X. G. Wen and P. A. Lee, *Phys. Rev. Lett.* **78**, 4111 (1997); L. B. Ioffe and A. J. Millis, cond-mat/0203348.
- [22] S. H. Pan, E. W. Hudson, A. K. Gupta, K. W. Ng, H. Eisaki, S. Uchida, and J. C. Davis, *Phys. Rev. Lett.* **85**, 1536 (2000).